Measurements and comparison of low frequency noise in *npn* and *pnp* polysilicon emitter bipolar junction transistors

M. Jamal Deen[a] and S. Rumyantsev
School of Engineering Science, Simon Fraser University, Burnaby, British Columbia, Canada V5A 1S6

R. Bashir and R. Taylor
National Semiconductor Corp., 2900 Semiconductor Drive, Santa Clara, California 95052-8090

(Received 21 October 1997; accepted for publication 30 March 1998)

Low frequency noise characteristics of new high voltage, high performance complementary polysilicon emitter bipolar transistors have been studied. The influence of the base biasing resistance, emitter geometry, and temperature on the noise spectra are discussed. The *npn* transistors studied exhibited $1/f$ and shot noise. The *pnp* transistors, on the other hand, are characterized by significant generation-recombination noise contributions to the total noise. For both types of transistors, the measured output noise is determined primarily by the noise sources in the polysilicon–monosilicon interface. The level of the $1/f$ noise is proportional to the square of the base current (I_B^2) for both *npn* and *pnp* transistors. The contribution of the $1/f$ noise in the collector current is also estimated. The magnitude of the $1/f$ noise normalized to the square of the base current for devices with different emitter areas was found to be inversely proportional to the emitter area, but for the transistors with a large ratio of emitter perimeter to emitter area, the contribution of noise sources located in the emitter perimeter may be significant. For both *pnp* and *npn* transistors, $1/f$ noise was found to be independent of temperature, and for *pnp* transistors, generation-recombination noise decreases with increasing temperature. © *1998 American Institute of Physics.* [S0021-8979(98)03413-6]

I. INTRODUCTION

Polysilicon emitter bipolar transistors are now widely used in analog circuits because of their low noise, high current, high β-early voltage product, and high frequency properties. The use of polysilicon emitter bipolar fabrication technology allows one to fabricate transistors with very small emitter areas in the sub-μm^2 range, and with very high unity gain frequencies of tens of GHz. However, as the transistors are made smaller, their low frequency noise increases. Even though the noise is at low frequencies, it can affect the high frequency performance of bipolar circuits, for example, the phase noise in oscillators is related to its low frequency noise. The phase noise in oscillators can limit the channel frequency spacing in communication systems. In addition, the low frequency noise can be upconverted to affect the high frequency performance of mixers. Also, noise sets the lower limit for signal detection in electronic systems.

To date, there are numerous articles that have been published on the low and high frequency noise characteristics of polysilicon emitter *npn* bipolar transistors.[1–15] A review of some of the literature on low frequency noise in *npn* transistors was given in Ref. 10. However, all these articles and their references report on low frequency noise only in *npn* polysilicon emitter bipolar transistors. To the best of our knowledge, there is no published information on low frequency noise on polysilicon emitter *pnp* bipolar transistors.

At low frequencies below 1–10 kHz, the noise in bipolar transistors is $f^{-\gamma}$ type, with γ typically in the range 0.85–1.1, in which case, it is referred to as $1/f$ noise. However, there are reports of γ values greater than 1.4.[11] Others[3] have reported generation-recombination (g-r) noise in the same frequency range as $f^{-\gamma}$ type noise, and even burst noise[11,12] was observed. At frequencies greater than 1–10 kHz, the shot noise of the base current[16–18] usually predominates if the level of $f^{-\gamma}$ type noise is low enough.

To date, most of the publications on low frequency noise in bipolar transistors in a common-emitter configuration suggests that the noise is associated with the base current.[1–14] At medium to high base currents that are typically used in normal bipolar operation, the spectral noise density of the base current fluctuations is usually proportional to the square of the base current, that is, $S_I \sim I_B^2$.[1–4,10,13] A stronger base current dependence current $S_I \sim I_B^3$ was also reported in Ref. 19. At low base current densities, the base current noise spectral density is sometimes given by $S_I \sim I_B$.[4,10,19,20]

Investigations of transistors with different properties of interfacial layers[1,7,13] show that the thin interfacial oxide layer between the polysilicon–silicon interface produces the main contribution to the noise when $S_I \sim I_B^2$. In Ref. 2, it was shown that hot electron stress by applying a sufficiently high reverse bias to the base–emitter junction increases only the noise which corresponds to $S_I \sim I_B$ part of the S_I versus I_B dependence. However, the hot electron degradation of transistors in Ref. 4 and 8 resulted in an increase in the low frequency noise over the entire range of base currents, even for minimal stress. These results indicate the possible different nature of low frequency noise for different base currents, and for transistors fabricated in different facilities. Also, the

[a]Electronic mail: jamal@cs.sfu.ca

0021-8979/98/84(1)/625/9/$15.00 © 1998 American Institute of Physics

Downloaded 05 Oct 2003 to 128.46.200.195. Redistribution subject to AIP license or copyright, see http://ojps.aip.org/japo/japcr.jsp

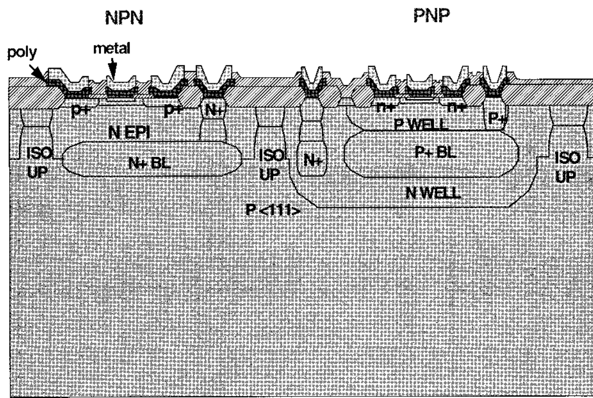

FIG. 1. Schematic cross-sectional view of the complementary *npn* and *pnp* polysilicon emitter bipolar transistors.

nature of low frequency noise may also be different for *npn* and *pnp* transistors.

Recently, a new complementary bipolar transistor technology was developed for the realization of high frequency, high voltage analog circuits.[21] Therefore, the purpose of this article is to measure and compare the low frequency noise properties of these new *npn* and *pnp* polysilicon emitter bipolar junction transistors.

II. DEVICES STUDIED

The transistors used in this study were fabricated on a polysilicon emitter complementary bipolar technology optimized for high speed and high β-early voltage product with BV_{ceo} greater than 85 V. The devices are nonself-aligned for ease of manufacturability. The base dopants are implanted through a pad oxide and the emitter is formed through diffusion from a polysilicon layer. The extrinsic base contacts are also made through diffusion from a poly-silicon layer. The poly–silicon/silicon interface is optimized for minimization of the interfacial oxide and improve matching of the devices.[21] A schematic cross-sectional view of the *npn* and *pnp* transistors studied is shown in Fig. 1.

The devices are vertically integrated *npn* and *pnp* transistors made using polysilicon emitter technology and are junction isolated. All isolation breakdown voltages for the *npn* and *pnp* are greater than 85 and 95 V for the *npn* and *pnp* transistors, respectively. Their unity-gain frequencies are 2 GHz for the *npn* and 1.6 GHz for the *pnp* transistors. For several transistors measured, constant current gain of 100 to 150 for the *npn*, and 30 to 100 for the *pnp*, was obtained for about seven decades of current variation.

The emitter geometries are rectangular with areas of 2×4, 4×20, and 2×40 μm^2, so their emitter perimeter (P_E) to emitter area (A_E) ratio varied from 0.6 to 1.5 μm^{-1}.

III. EXPERIMENTAL PROCEDURE AND DEVICE CURRENT–VOLTAGE CHARACTERISTICS

The devices studied were biased in the common emitter configuration, as shown in Fig. 2. Inside the dashed box in Fig. 2 is the simplified low-frequency equivalent circuit of the bipolar transistor. The noise properties of the transistor

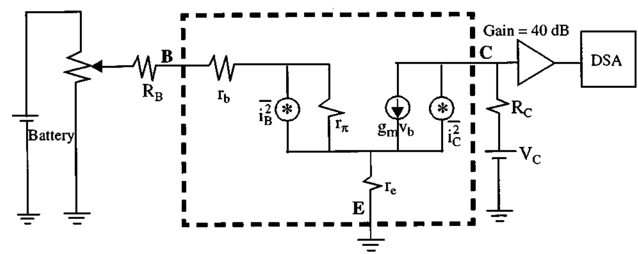

FIG. 2. Circuit used to bias the transistors for noise measurements. The simplified low frequency equivalent circuit of the bipolar transistor is shown inside the dashed box.

are represented by the two noise power generators $\bar{i_B^2}$ and $\bar{i_C^2}$. In Refs. 2, 10, and 20, it was shown that the internal base resistance r_b and emitter resistance r_e can contribute to the noise characteristics of the devices. However, for the devices we have studied, the values of r_b and r_e are very low, and they were significantly less than the base biasing resistance R_B and the base-emitter resistance $r_\pi \sim \Delta V_B/\Delta I_B$. Because of this, we can neglect the noise contributions of the base and emitter resistances of the transistor.

The base and emitter resistances of the transistors were determined from scattering parameters measurements from 50 to 350 MHz using the standard impedance circle technique. The base-emitter bias was adjusted between 0.8 and 0.95 V for the *npn* transistors and 0.7 to 0.85 V for the *pnp* transistors. After r_b and r_e were extracted, dc current–voltage ($I-V$) measurements were made (Gummel characteristics) and these experimental results were used to check the accuracy of the extracted base and emitter resistances. Good agreement was obtained. The values of r_e for *npn* and *pnp* transistors are $r_e=146$ and $r_e=260\ \Omega\ \mu$m^2, respectively. The base resistance at typical operating current levels (R_{BM} is SPICE model) were 50 (*npn*) and 102 Ω (*pnp*) for the 8 μm^2 transistors, and 10 (*npn*) and 20.5 Ω (*pnp*) for the 80 μm^2 transistors.

The noise signal from the collector biasing resistance R_C was amplified with a PAR 113 low noise voltage amplifier, and then measured with a HP 3561 dynamic signal analyzer. Batteries were used to bias the base and collector terminals. The collector biasing resistance R_C used was 2.5 kΩ, and this was much smaller than the output resistance of the transistor. All measurements were performed on wafer using a shielded wafer probing system. The influence of the point contacts on the noise measurements has been checked using different contact pressures of the needles on the aluminum pads. The contact pressures used had negligible influence on the noise measured.

From the equivalent circuit representation shown in Fig. 2, the spectral noise density of voltage fluctuations across resistance R_C can be expressed as

$$\frac{S_{V_C}}{R_C^2}=\left(\frac{R_B+r_b+r_e}{R_B+r_b+r_\pi+(\beta+1)r_e}\right)^2 \cdot\beta^2\cdot\left(S_{i_B}+\frac{4kT}{R_B+r_b+r_e}+2qI_B\right)+S_C, \tag{1a}$$

where

Downloaded 05 Oct 2003 to 128.46.200.195. Redistribution subject to AIP license or copyright, see http://ojps.aip.org/japo/japcr.jsp

$$S_C=\left(\frac{R_B+r_b+r_\pi+r_e}{R_B+r_b+r_\pi+(\beta+1)r_e}\right)^2(S_{i_C}+2qI_C)+\frac{4kT}{R_C}. \tag{1b}$$

Here $\beta=\Delta I_C/\Delta I_B$ is the dynamic current gain, I_B and I_C are the base and collector currents, respectively, S_{i_B} and S_{i_C} are the spectral noise densities of the low frequency noise (both $1/f$ and generation recombination components) associated with the base and collector noise generators, r_b and r_e are the internal base and emitter resistances, $r_\pi\sim\Delta V_B/\Delta I_B$ is the base-emitter resistance. Noise measurements were made using base biasing resistance R_B between 200 kΩ and 10 MΩ typically, and between 100 Ω and 10 MΩ for a special series of experiments.

For the *npn* and *pnp* transistors, possible degradation effects of both the Gummel characteristics as well as the noise spectra due to the biasing used or time of several days were investigated. No measurable effects were obtained.

The Gummel characteristics of both *npn* and *pnp* transistors are shown in Figs. 3(a) and 3(b). It is seen that the current–voltage characteristics of both types of transistors are excellent. Gummel plots of transistors with different emitter geometries (2×40 and 4×20 μm^2) but the same area were identical. Note that very little dependence of the $I-V$ or noise spectra on the collector voltage in the range of 5–14 V were measured. For all *npn* and *pnp* transistors except one studied, the ideality factor was 1 with no measurable recombination currents for base currents as low as 1 pA. Only two transistors showed recombination current. We call one of these transistors with base recombination current **transistor R** for identification later [see Fig. 3(b)].

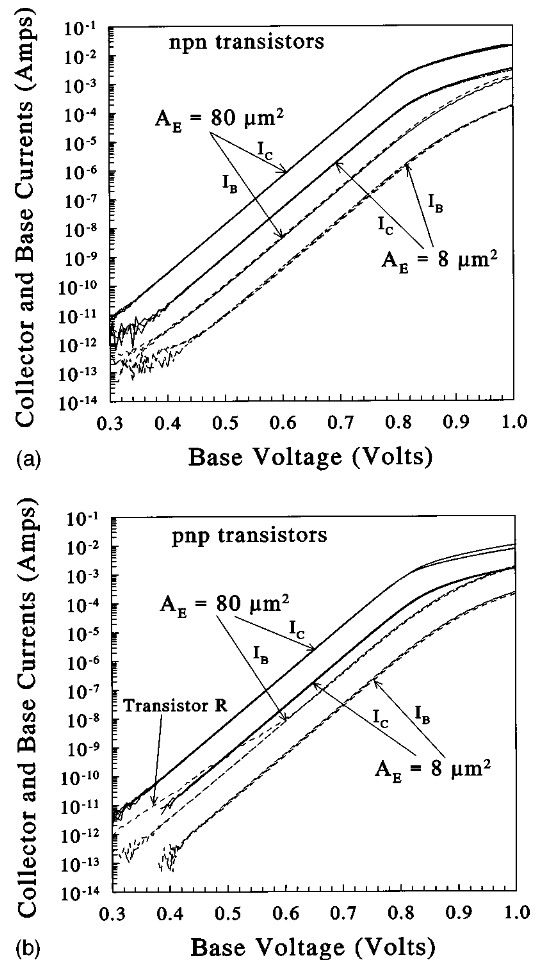

FIG. 3. Gummel plots of *npn* (a) and *pnp* (b) transistors. The characteristics for several transistors of each area and each type are plotted.

IV. RESULTS AND DISCUSSIONS

A. Low frequency noise spectra

The noise spectra described in this section were measured with the base biasing resistance $R_B\gg r_\pi$, $(\beta+1)r_e$, or r_b. In order to satisfy this condition over a wide range of base currents, biasing resistance R_B in the range 2×10^5 Ω $<R_B<10^7$ Ω was used. In this case, the spectral noise density of the base current fluctuations (S_{i_B}) is multiplied by β^2 [see Eq. (1)], and the collector noise sources can be neglected. The thermal noise $[4kT/(R_B+r_b+r_e)]$ can also be neglected because it is significantly less that the shot noise $(2qI_B)$. In this case, for the input noise spectral density S_I, we get,

$$S_I=\frac{S_{V_C}}{\beta^2R_C^2}\approx S_{i_B}+2qI_B. \tag{2}$$

Typical noise spectra S_I for *npn* transistors with emitter area 4×20 μm^2 are shown in Fig. 4(a). The solid lines show the results according to the calculations using Eq. (2). The dependence of S_{i_B} on current and frequency (for the case of $1/f$ and g-r noise) is expressed as

$$S_{i_B}=\frac{K_F\cdot I_B^{A_F}}{f^\gamma}+\sum_i\frac{B_i\tau_i}{1+(2\pi f\tau_i)}, \tag{3}$$

where $A_F=2$, $\gamma=1$, and K_F represents the amplitude of the $1/f$ noise normalized to a frequency of 1 Hz and a current of 1 A, B_i represents the amplitudes of the g-r noise components, τ_i are the characteristic time constants of g-r noise components (A_F, γ, and K_F are parameters typically used in SPICE modeling of $1/f$ noise).

The solid curves in Fig. 4(a) are calculated using Eqs. (2) and (3), assuming no contribution of the g-r noise ($B_i=0$). Only K_F values were used to fit experimental data over the frequency range where $1/f$ noise predominates. No fitting for the frequency independent shot noise [second term in Eq. (2)] was used. It is seen from Fig. 4(a) that the noise observed in *npn* transistors is described well as a sum of $1/f$ and shot noise of the base current.

Only for a few *npn* transistors did we observe a small contribution of generation-recombination noise. It must be pointed out that this low level of generation-recombination noise is typical of modern *npn* polysilicon emitter bipolar transistors, and has been reported by others, see Refs. 2 and 3 for example.

In contrast the noise spectra of *pnp* transistors had a significant contribution of g-r noise and were characterized by different noise level and different current dependencies of the spectra. Figures 4(b) and 4(c) show the noise spectra for

Downloaded 05 Oct 2003 to 128.46.200.195. Redistribution subject to AIP license or copyright, see http://ojps.aip.org/japo/japcr.jsp

two *pnp* transistors with the same emitter area, but different emitter perimeter.

For the transistor in Fig. 4(b) at the base current $I_B = 0.33\ \mu A$, there is no distinguishable contribution of the g-r noise to the spectra which is well described as a sum of $1/f$ and shot noise [$B_i = 0$ in Eq. (3)]. At higher currents, the significant contribution of g-r noise was observed for this transistor. It is important to note, that at different currents, the amplitude of the g-r noise relative to the $1/f$ noise and the corner frequencies $f_i = 1/2\pi\tau_i$ are different. Two corner frequencies are shown in Fig. 4(b) as examples. The noise spectra at $I_B = 1.1$ and $I_B = 1.94\ \mu A$ are well represented as a sum of $1/f$ noise, shot noise, and one g-r noise component. For the spectra at $I_B = 14$ and $I_B = 48\ \mu A$, two distinguishable g-r components were observed.

The noise spectra shown in Fig. 4(c) are quite different. At low currents $I_B = 0.18$ and $I_B = 0.33\ \mu A$ the noise spectra are close to $1/f^{0.5}$ law (the noise spectra with $\gamma < 1$ have been observed before—see for example Ref. 22). This kind of spectrum can be approximated by multiple g-r components. For example, the curves for $I_B = 0.18$ and $I_B = 0.33\ \mu A$ calculated according Eqs. (2) and (3) contain 3 and 4 g-r components, respectively. At higher currents, the noise spectra can be fitted well by the sum of $1/f$ and one ($I_B = 1.1$ and $I_B = 14\ \mu A$) or two ($I_B = 48\ \mu A$) g-r noise components. However the value of K_F for the spectrum at $I_B = 1.1\ \mu A$ is very high [see Fig. 4(c) caption]. This probably means that the g-r components which contribute to the spectra at $I_B = 0.18$ and $I_B = 0.33\ \mu A$ can also contribute to the spectrum at $I_B = 1.1\ \mu A$, but result in $1/f$ like spectrum.

In semiconductor resistors, the values K_F, B_i' (where $B_i' = B_i/I^2$), τ_i in Eq. (3) do not usually depend on current and for the whole spectrum the law $S_I \sim I^2$ is valid. With an increase in the current, the noise spectral density S_I increases proportionally at all frequencies. However, a quite different situation was observed in *pnp* transistors. For all transistors, the dependence of the shape of the spectra on the base current was observed. In other words, the $1/f$ noise and g-r noise are characterized by different current dependencies. One of the possible reason of this phenomena may be the dependence of B_i' and τ_i values on the base current, that is, B_i is not proportional to the square of the base current.

The dependence of the g-r noise on current has been studied in AlGaAs/GaAs heterojunction bipolar transistors (HBTs).[23] In these HBTs, it was found that the corner frequency of the g-r noise $f = 1/2\pi\tau$ moves to higher values as the base current increases. Since the base voltage V_B also increases with base current, it is probable that just this V_B increase results in a shift of the characteristic frequencies to higher values. The B_i' and τ_i values are determined by the occupancy of the level which is responsible for g-r noise (see, for example, Refs. 6, 24 and 25). If the level is located in the base-emitter *p-n* junction, then increasing the base voltage leads to a change of the energy difference between the defect energy level and the Fermi level, and consequently to a modification of the level occupancy and g-r noise spectra.[6,24,25]

As discussed above, the *pnp* transistors are characterized by a different level of noise. Even a couple of transistors

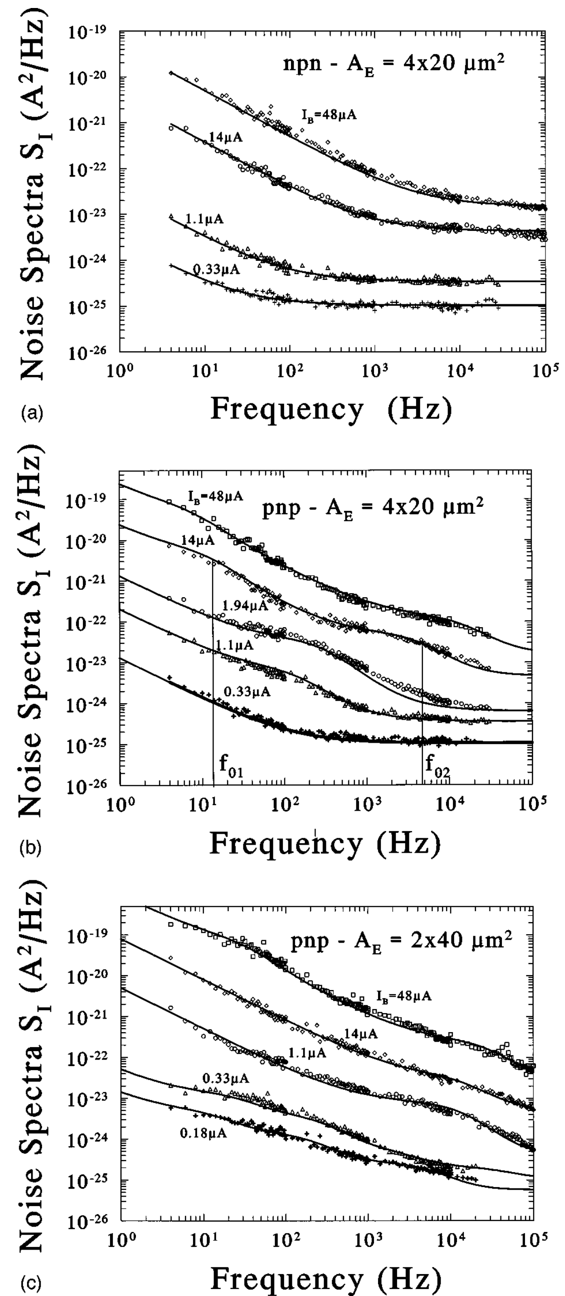

FIG. 4. Input noise spectra $S_I = S_{V_C}/(\beta^2 R_C^2)$ for different transistors measured under the condition of the base biasing resistance $R_B \gg r_\pi$ for different base currents I_B's. The lines are calculations using Eq. (2); (a) Noise spectra for a *npn* transistor with emitter geometry 4 μm×20 μm. $I_B = 48\ \mu A - K_F = 2.2\times10^{-11}$; $I_B = 14\ \mu A - K_F = 1.9\times10^{-11}$; $I_B = 1.1\ \mu A - K_F = 2.4\times10^{-11}$; $I_B = 0.33\ \mu A - K_F = 2.7\times10^{-11}$; (b) Noise spectra for a *pnp* transistor with emitter geometry 2 μm×40 μm. Note that these spectra show clear g-r noise, in addition to shot noise and $1/f$ noise. Note that $f_i = 1/2\pi\tau_i$. $I_B = 48\ \mu A - K_F = 0.9\times10^{-10}$, $f_1 = 8$ Hz, $B_1 = 2\times10^{-18}$; $f_2 = 16$ kHz, $B_2 = 1\times10^{-17}$; $I_B = 14\ \mu A - K_F = 1.0\times10^{-10}$, $f_1 = 13$ Hz, $B_1 = 3.2\times10^{-19}$; $f_2 = 4.8$ kHz, $B_2 = 1.2\times10^{-18}$; $I_B = 1.94\ \mu A - K_F = 3.4\times10^{-10}$, $f_1 = 320$ Hz, $B_1 = 6\times10^{-20}$; $I_B = 1.1\ \mu A - K_F = 1.6\times10^{-10}$, $f_1 = 160$ Hz, $B_1 = 5\times10^{-21}$; $I_B = 0.33\ \mu A - K_F = 1.2\times10^{-10}$; (c) Noise spectra for a *pnp* transistor with emitter geometry 4 μm×20 μm. Note that these spectra show clear g-r noise, in addition to shot noise and $1/f$ noise. Note that $f_i = 1/2\pi\tau_i$. $I_B = 48\ \mu A - K_F = 3.9\times10^{-10}$, $f_1 = 32$ Hz, $B_1 = 1\times10^{-17}$; $f_2 = 32$ kHz, $B_2 = 4\times10^{-17}$; $I_B = 14\ \mu A - K_F = 4.0\times10^{-10}$, $f_1 = 16$ kHz, $B_1 = 2.5\times10^{-18}$; $I_B = 1.1\ \mu A - K_F = 4.0\times10^{-9}$, $f_1 = 14$ kHz, $B_1 = 6.3\times10^{-19}$; $I_B = 0.33\ \mu A - K_F = 3.0\times10^{-10}$, f_i(Hz)=32 Hz; 320 Hz; 3.2 kHz; 48 kHz, $B_i = 1.6\times10^{-21}$, 6×10^{-21}, 6×10^{-21}, 3×10^{-20}, respectively; $I_B = 0.33\ \mu A - K_F = 1.2\times10^{-10}$; f_i(Hz): 16 Hz; 240 Hz; 6.4 kHz, B_i: 3×10^{-22}, 1.5×10^{-21}, 8×10^{-21}, respectively.

Downloaded 05 Oct 2003 to 128.46.200.195. Redistribution subject to AIP license or copyright, see http://ojps.aip.org/japo/japcr.jsp

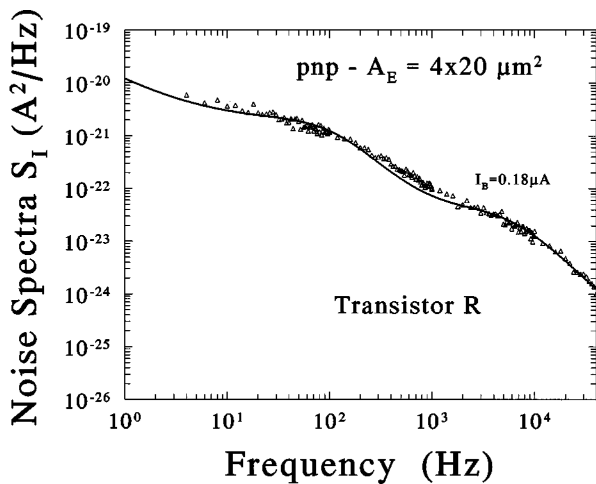

FIG. 5. Noise spectra $S_I = S_{V_C}/(\beta^2 R_C^2)$ of the abnormally high noise observed in the transistor R. $K_F = 3\times10^{-7}$, $f_1 = 110$ Hz, $B_1 = 1.4\times10^{-18}$; $f_2 = 6.4$ kHz, $B_2 = 1.6\times10^{-18}$.

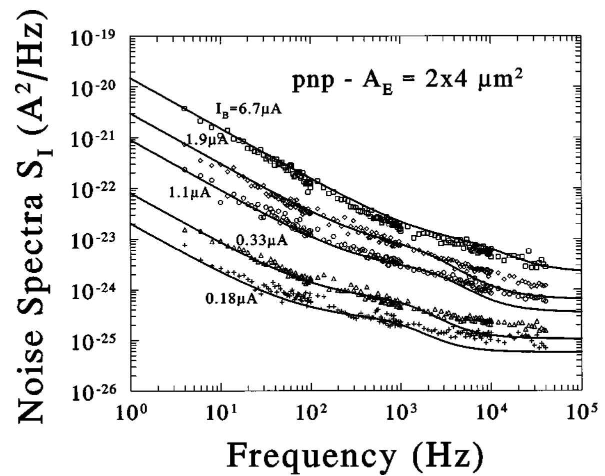

FIG. 6. Noise spectra $S_I = S_{V_C}/(\beta^2 R_C^2)$ for the small pnp transistor of emitter geometry 2×4 μm². $I_B = 6.7$ μA$-K_F = 3.3\times10^{-10}$, $f_1 = 11$ kHz, $B_1 = 3.5\times10^{-19}$; $I_B = 1.94$ μA$-K_F = 7\times10^{-10}$, $f_1 = 2.4$ kHz, $B_1 = 7.5\times10^{-20}$; $I_B = 1.1$ μA$-K_F = 7.4\times10^{-10}$, $f_1 = 3.2$ kHz, $B_1 = 4\times10^{-20}$; $I_B = 0.33$ μA$-K_F = 7.3\times10^{-10}$, $f_1 = 1.6$ kHz, $B_1 = 5\times10^{-21}$; $I_B = 0.18$ μA $-K_F = 6.2\times10^{-10}$, $f_1 = 1.3$ kHz, $B_1 = 1.6\times10^{-21}$.

exhibited abnormally high levels of noise. One of the example is transistor R with nonideal current–voltage characteristic shown in Fig. 3(b). The noise spectra for transistor R is shown in Fig. 5 for the same current $I_B = 0.18$ μA as one of the spectra in Fig. 4(c).

One of the reasons why pnp transistors under investigations demonstrated significantly different level of the noise may be that the transistors in different parts of the wafer were of slightly different technological conditions. In order to check this assumption we measured noise in the central and peripheral parts of the wafer. However the transistor's noise (for transistors of the same emitter geometry) was independent of its position on the wafer. That is, even neighboring pnp transistors (of the same geometry) exhibited significantly different noise spectra.

In spite of a large difference in the noise among the pnp transistors, the current–voltage characteristics for all pnp transistors except two are practically identical, the only exceptions are the transistors for which the base current was nonideal (**transistor R**), and this is shown in Fig. 3(b). This confirms the fact that noise measurement is a very sensitive technique for investigating the quality of materials and devices,[26–28] and for determining deep level parameters with low concentrations.[25,29]

The typical noise spectra for small pnp transistors at different base current are shown in Fig. 6 For the small area pnp transistors, the noise spectra at low frequencies less than 10–100 Hz had the form of $1/f$ noise. At higher frequencies the spectra became more flat ($S_I \sim f^{-0.3 \text{ to } -0.5}$) and they can be fitted only by multiple g-r components. In order to demonstrate the last fact, only one g-r component was used for every curve in Fig. 6.

B. Dependence of low frequency noise on the base biasing resistance

In order to prove that the main contribution to the output noise is due to the amplified noise in the base-emitter junction [see Eq. (1)] under the condition that $R_B \gg r_\pi$, noise measurements were performed with different base biasing resistances R_B. Figure 7 shows the dependence of the output noise S_{V_C} on the base biasing resistance for a npn transistor with emitter area of 2×4 μm² [Fig. 7(a)], and for a pnp transistor with emitter area of 2×40 μm² [Fig. 7(b)]. The symbols show the experimental results and the lines show the calculated results using Eq. (1). The value of the transistor's base resistance r_b is assumed to be much smaller than either R_B or r_π, that is, $r_b \ll R_B$, r_π. The values of the input resistance $r_\pi \approx \Delta V_B/\Delta I_B$ were determined directly from the Gummel plots [Fig. 3], and are 5 and 20 kΩ at 6 and 1 μA base currents, respectively. For the small transistors (2×4 μm²), significant contribution to the dependence of S_{V_C} versus R_B gives the term $(\beta+1)r_e$.

The solid triangles and solid lines in Fig. 7 show the results at 10 Hz where $1/f$ noise dominates. The bold circles and dashed curves show the results at 10 kHz, where at all values of R_B, the frequency independent shot noise dominates. The small difference in output shot noise at $R_B > 10^5$ Ω for $I_B = 1$ and 6 μA in Fig. 7(a) is due to the current gain β decreasing as I_B increases. A rather significant decrease of the noise as R_B decreases was experimentally observed, with good qualitative agreement to the calculations. Therefore, measurements under the condition that $R_B \gg r_\pi$ shows only amplified base noise. This conclusion agrees with similar measurements and conclusions for npn transistors made in Ref. 1.

In order to fit the experimental data at low values of R_B, the collector $1/f$ noise was taken into account. This allowed us to estimate the values of K_F for the collector $1/f$ noise. This calculation gives $K_F \sim 10^{-9}$ for npn transistors, and $K_F \sim 10^{-10}$ for pnp transistors. However, the pnp transistors discussed in this section have emitter areas that are ten times larger than the npn transistors. Assuming that the K_F values are inversely proportional to emitter area, then we can conclude that the collector $1/f$ noise in both npn and pnp transistors are of similar magnitude.

Downloaded 05 Oct 2003 to 128.46.200.195. Redistribution subject to AIP license or copyright, see http://ojps.aip.org/japo/japcr.jsp

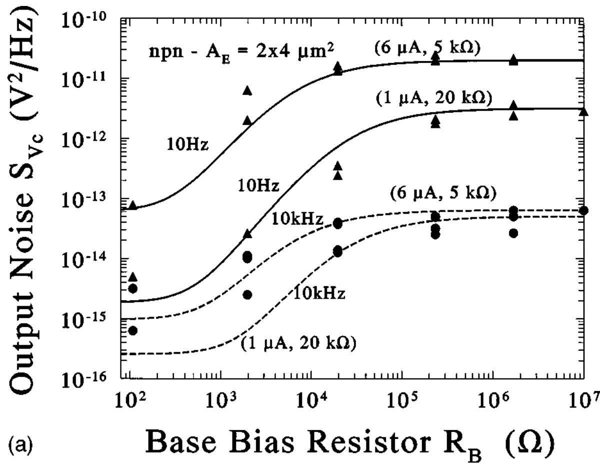

(a)

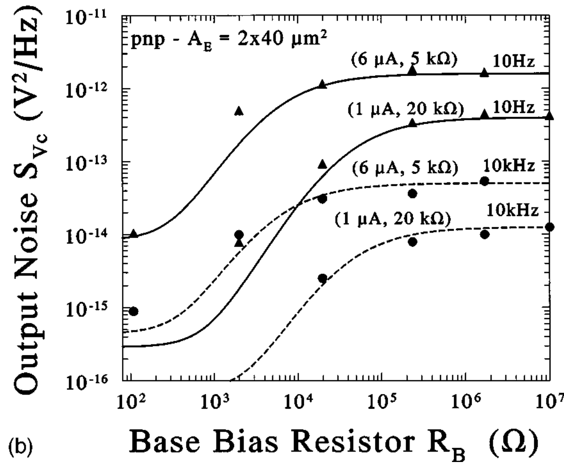

(b)

FIG. 7. The dependence of the output noise S_{V_C} on the base biasing resistance R_B for (a) *npn* and (b) *pnp* transistors. The bold triangles and bold circles show the results of measurements at 10 Hz and 10 kHz, respectively. The lines are calculations using Eq. (1). The base currents I_B and the input resistance dV_B/dI_B are given in the figure.

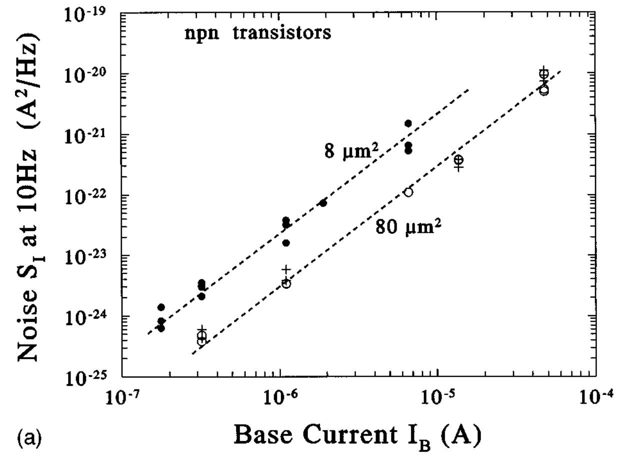

(a)

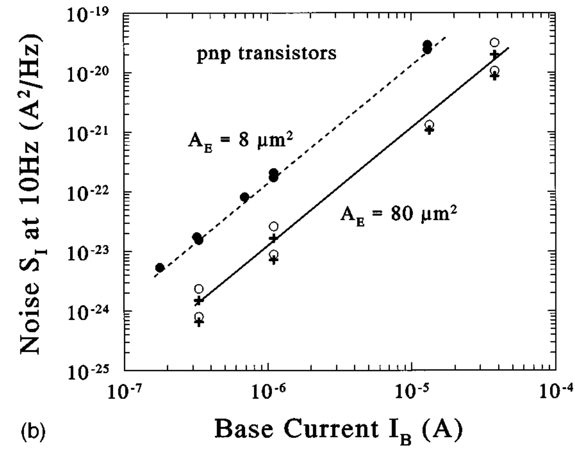

(b)

FIG. 8. Dependence of noise spectra $S_I=S_{V_C}/(\beta^2R_C^2)$ at 10 Hz, on the base current for (a) *npn* and (b) *pnp* transistors. The lines show the variation $S_I\propto I^2$ since $1/f$ noise is dominant at 10 Hz. The bold circles show the measured data for transistors with emitter geometry 8 μm². The open circles and crosses show measured results for transistors with emitter geometries 2 μm×40 μm and 4 μm×20 μm, respectively. For the *pnp* transistors, the g-r noise contribution at 10 Hz was subtracted from the measured spectra.

C. Current dependence of the low frequency noise

Noise measurements at different base currents were performed under the condition $R_B \gg r_\pi$. Figure 8(a) shows the current dependence of the noise measured at 10 Hz from *npn* transistors with different emitter areas. It is seen that for both the small and large devices, that

$$S_I=\frac{S_{V_C}}{\beta^2\cdot R_C^2}\propto I_B^2. \tag{4}$$

Figure 9 shows the dependence of the static (β_S) and dynamic (β) current gain on the base current. For base currents less than 10 μA, $\beta_S\cong\beta$ and the spectral noise density for collector current fluctuations S_{V_C}/R_C^2 is proportional to I_C^2. However, for base currents larger than 10 μA, $\beta_S>\beta$ and S_{V_C}/R_C^2 variation with collector current depends on β/β_S. That is, if Eq. (4) holds, then

$$\frac{S_{V_C}}{R_C^2}\sim\frac{I_C^2\cdot\beta^2}{\beta_S^2}. \tag{5}$$

Therefore, at high base currents, the spectral noise density of the base current fluctuations is proportional to I_B^2, but the spectral noise density of the collector current fluctuations is not proportional to I_C^2.

Figure 8(b) shows the dependence of $S_I=S_{V_C}/(\beta^2R_C^2)$ on the base current for *pnp* transistors. Because *pnp* transistors were characterized by significant contribution of g-r noise to the measured spectra, we subtracted out the g-r noise and kept only the $1/f$ noise and shot noise. That is, in Fig. 8(b), only noise data for the $1/f$ component as a function of base current for devices of two different areas are shown. It is seen from Fig. 8(b) that for the $1/f$ noise, $S_{I_B}\sim I_B^2$ with good accuracy.

D. Dependence of low frequency noise on the emitter geometry

It is known that if the noise is produced by independent fluctuators homogeneously distributed in the same part of the device, that the relative spectral noise density of voltage or current fluctuations is inversely proportional to the size of this element. For example, the spectral noise density of bulk

Downloaded 05 Oct 2003 to 128.46.200.195. Redistribution subject to AIP license or copyright, see http://ojps.aip.org/japo/japcr.jsp

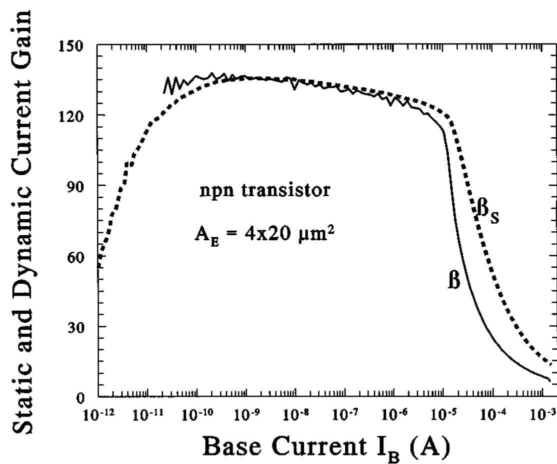

FIG. 9. Variation of the dynamic (β) and static (β_S) current gain on base current for a *npn* transistor with emitter geometry 4 μm×20 μm.

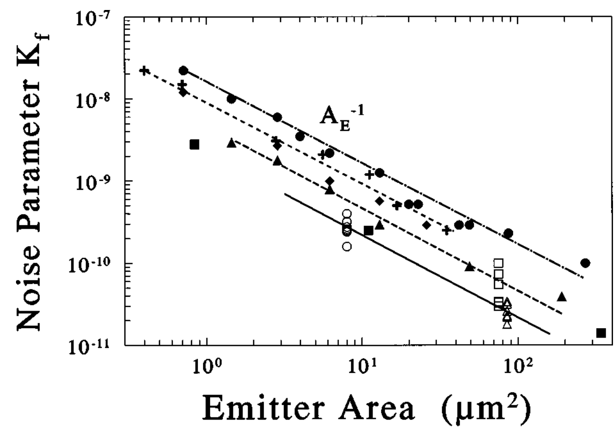

FIG. 10. Dependence of the noise parameter K_F on the emitter area for *npn* transistors. The meanings of the symbols are as follows: Bold circles-unmasked emitter (Ref. 14); bold diamond-masked emitter (Ref. 14); bold squares (Ref. 2); bold triangles (Ref. 3); bold crosses (Ref. 32); open symbols-present work. Note that the 80 μm^2 transistors have been offset for clarity (the open squares are for 2×40 μm^2 and the open triangles are for 4×20 μm^2).

generation-recombination noise is inversely proportional to the volume.[24] In accordance with the Hooge's expression,[30] the relative spectral noise density of the $1/f$ noise is inversely proportional to the total number of carriers, so that for a homogeneous semiconductor, this leads to $1/f$ noise being inversely proportional to the volume. This empirical observation can be used in measurements of noise in semiconductors and semiconductor devices with different relationships of volume to surface area, or surface area to perimeter in an attempt to localize the noise sources.

There have been some previous attempts to measure the $1/f$ noise in polysilicon emitter bipolar transistors with different emitter areas A_E,[2,3,15] different emitter perimeters P_E,[3,15] and different area-to-perimeter ratios A_E/P_E.[3,14,15] It was shown[2,3,14,15] that the relative spectral noise density of the base current fluctuations normalized to 1 Hz is given by $K_F = S_I/(I^2 \cdot f)$, varies inversely with emitter area A_E. Figure 10 shows the dependence of K_F on emitter area for our *npn* transistors, as well as those in Refs. 2, 3, 14 and 15 It is seen that all *npn* transistors studied here demonstrated a low level of $1/f$ noise. The dependence of noise on emitter area may be described by $K_F \approx A_E^{-1}$. However, three transistors with emitter perimeter of 84 μm have a slightly higher noise, and this indicates that there is some contribution of the noise sources located in the emitter perimeter to the total transistor noise.

E. Temperature dependence of the low frequency noise

Low frequency noise, and current–voltage characteristics were measured for both *npn* and *pnp* transistors at temperatures between 22 and 85 °C. Figure 11 shows the dependence of the dynamic current gain β on base current for *pnp* transistors at different temperatures. It is seen that for the range of base currents for which β does not change with I_B, that β increases as the temperature increases. This is the usual dependence of β on temperature for conventional[31] and polysilicon emitter bipolar transistors.[32,33] The Gummel characteristics of both types of transistors studied were close to ideal characteristics, and at 85 °C, the ideality factor is close to its ideal value to within 5%.

Figure 12 shows the noise spectra at 22 and 85 °C for *pnp* transistors for which, g-r noise at room temperature was clearly observed. It is seen that with increase in temperature, the level of g-r noise decreases at all frequencies. Measurements of noise spectra at temperatures between 22 and 85 °C show that the noise decreases monotonically as the temperature increases.[26]

As was discussed before, for *npn* transistors, $1/f$ and shot noise dominates the spectra at room temperature. No temperature dependence of the output noise was observed for these transistors. This agrees with the experimental results in Ref. 13, and supports the idea that $1/f$ noise in polysilicon emitter bipolar transistors is due to fluctuations in the tunneling probability across the interfacial oxide barrier at the polysilicon–monocrystalline silicon interface of the emitter. In Refs. 3 and 6, the temperature dependence of the low frequency noise was also measured in polysilicon emitter

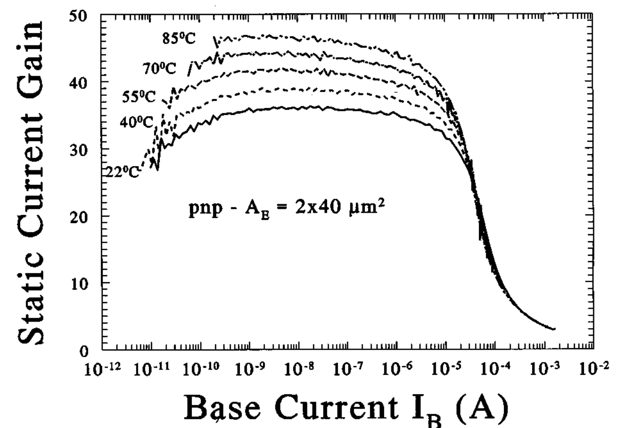

FIG. 11. Dependence of the static current gain on the base current for *pnp* transistors at different temperatures.

Downloaded 05 Oct 2003 to 128.46.200.195. Redistribution subject to AIP license or copyright, see http://ojps.aip.org/japo/japcr.jsp

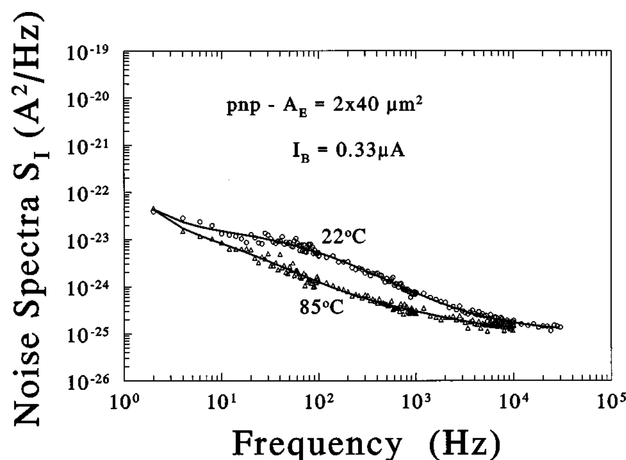

FIG. 12. Noise spectra S_I for a *pnp* transistor with emitter geometry 2 μm×40 μm at 22 and 85 °C.

bipolar transistors. However, the noise in Refs. 3 and 6 was attributed to g-r noise, for which the expected strong temperature dependence was measured.

V. CONCLUSIONS

Low frequency noise in new complementary high voltage and high frequency polysilicon emitter *npn* and *pnp* bipolar transistors have been investigated. The low frequency noise spectra of *npn* transistors consisted of $1/f$ noise at lower frequencies and shot noise which predominates at frequencies higher than ~1 kHz. For a few *npn* transistors, weak generation-recombination noise was observed.

In contrast, the low frequency noise spectra of *pnp* transistors have a significant contribution from generation-recombination (g-r) noise. The relative contribution of the g-r components to the total noise depends on the base current. This is clearly indicated by the dependence of the shape of the noise spectra on the base current. The different dependence of $1/f$ and g-r noise on the base current reflects a different nature and also a possibly different location of these two types of low frequency noise sources in *pnp* transistors. For the small transistors (emitter area$=2\times4\ \mu\text{m}^2$), the $f^{-\gamma}$ type of noise with $\gamma\sim0.3$ to 0.5 was observed at low base currents.

The measurements of the noise with different values of external base biasing resistances R_B was performed. Measurements with low values of R_B allowed us to estimate the collector current noise contribution to the total output noise. Under the condition that $R_B \gg r_\pi$, the main contribution to the output noise is due to the amplified noise of the base current. With $R_B \gg r_\pi$, the spectral noise density of output current fluctuations S_I is proportional to I_B^2 over the entire range of base currents studied. At high base currents, S_I is still proportional to I_B^2, but not to I_C^2 because the static current gain is higher than the dynamic current gain.

Low frequency noise was also measured at temperatures between 22 and 85 °C. Very little temperature dependence of the noise on temperature was observed for the *npn* transistors. The g-r noise observed in the *pnp* transistors decreases monotonically with increasing temperature. This indicates that the energy level(s) of the defect(s) responsible for the g-r noise is (are) located near or above the quasi-Fermi level at the temperature of measurement.

Finally, the dependence of the $1/f$ noise magnitude, measured with the K_F parameter, on the emitter area for *npn* transistors can be described by $K_F \sim A_E^{-1}$. Transistors with the same area, but larger perimeter exhibited a slightly higher noise level. This indicates that there is some contribution from noise sources located in the perimeter of the emitter. The *pnp* transistors have a large dispersion of the noise level, mainly because of the contribution of the g-r noise. However, the noise level of the *pnp* transistors are comparable to the noise of the *npn* transistors of the same emitter area, and are similar to published noise levels for *npn* transistors of similar areas.

ACKNOWLEDGMENTS

We gratefully acknowledge the support of National Semiconductor Corporation, Santa Clara, California, and the Natural Sciences and Engineering Research Council (NSERC) of Canada. We also acknowledge several useful discussions with Dr. X. Y. Chen, Engineering Science, Simon Fraser University (now at University of Tromso, Tromso, Norway). Finally, we thank Dr. Tracey L. Krakowski of National Semiconductor, Santa Clara, California for her assistance with the bipolar transistor parameters.

[1] E. Simoen, S. Decoutre, A. Cuthbertson, C. Claeys, and L. Deferm, IEEE Trans. Electron Devices **ED-43**, 2261 (1996).
[2] H. Markus and T. G. M. Kleinpenning, IEEE Trans. Electron Devices **ED-42**, 720 (1995).
[3] M. J. Deen, J. I. Ilowski, and P. Yang, J. Appl. Phys. **77**, 6278 (1995).
[4] A. Mounib, F. Balestra, N. Mathieu, J. Brini, G. Ghibaudo, A. Chovet, A. Chantre, and A. Nouailhat, IEEE Trans. Electron Devices **ED-42**, 1647 (1995).
[5] N. Siabi-Shahrivar, W. Redman-White, P. Ashburn, and H. A. Kemhadjian, Solid-State Electron. **38**, 389 (1995).
[6] A. Ng, M. J. Deen, and J. Ilowski, Can. J. Phys. **70**, 949 (1992).
[7] M. J. Deen, J. I. Ilowski, and P. Yang, *Proceedings of the 13th International Conference on Noise in Physical Systems and 1/f Fluctuations*, edited by V. Bareikis and R. Katilius (World Scientific, Singapore, 1995), pp. 454–457.
[8] M. Doan, Z. Buffet, and M. J. Deen, *Proceedings of the Symposium on the Degradation of Electronic Devices Due to Device Operation as Well as Crystalline and Process-Induced Defects*, edited by H. J. Quessnier, J. E. Chung, K. E. Bean, T. J. Shaffner, and H. Tsuya (The Electrochemical Society Press, Pennington, NJ, (1994), Vol. 94-1, pp. 235–241.
[9] M. J. Deen and J. J. Ilowski, *AIP Conference Proceedings 285—Noise in Physical Systems and 1/f Fluctuations (ICNF '93)*, edited by P. H. Handel and A. L. Chung (AIP, New York, 1993), pp. 216–219; A. Ng and M. J. Deen, *AIP Conference Proceedings 285—Quantum 1/f Noise & Other Low Frequency Fluctuations in Electronic Devices*, edited by P. H. Handel and A. L. Chung (AIP, New York, 1993), pp. 142–164.
[10] T. G. M. Kleinpenning, IEEE Trans. Electron Devices **ED-41**, 1981 (1994).
[11] P. F. Lu, J. Appl. Phys. **62**, 1335 (1987).
[12] T. G. M. Kleinpenning and A. J. Holden, *Proceedings of the 12th International Conference on Noise in Physical Systems and 1/f Fluctuations*, edited by T. Musha, S. Sato, and M. Yamamoto (Ohmsha, Tokyo, 1991), pp. 435–438.
[13] W. S. Lau, E. F. Choi, C. S. Foo, and W. C. Khoong, Jpn. J. Appl. Phys., Part 2 **31**, L1021 (1992).
[14] P. Linares, D. Celi, O. Roux-Dit-Buisson, G. Ghibaudo, and J. Chroboczek, Proceedings of the 14th International Conference on Noise in Physi-

Downloaded 05 Oct 2003 to 128.46.200.195. Redistribution subject to AIP license or copyright, see http://ojps.aip.org/japo/japcr.jsp

cal Systems and 1/f Fluctuations (14–18 July, 1997), Leuven, Belgium, pp. 181–184.
[15] X. Y. Chen, M. J. Deen, Z. X. Yan, and M. Schroter, Electron. Lett. **34**, 219 (1998).
[16] M. J. Deen, Can. J. Phys. **74**, 5200 (1996).
[17] M. J. Deen and J. J. Ilowski, Electron. Lett. **29**, 676 (1993).
[18] M. J. Deen, Proceedings of the First International Conference on Unsolved Problems of Noise (UPON '96), Szeged, Hungary, 3–7 September, 1996, pp. 199–204.
[19] A. H. Pawlikiewicz, A. van Der Ziel, G. S. Kousik, and C. M. Van Vliet, Solid-State Electron. **31**, 831 (1988).
[20] T. G. M. Kleinpenning, IEEE Trans. Electron Devices **ED-39**, 1501 (1991).
[21] R. Bashir, D. Chen, F. Hebert, J. DeSantis, A. Ramde, S. Hobrecht, H. You, P. Maghsoudina, P. Meng, and R. R. Razouk, Proceedings of ESSDERC '96 (1996), pp. 217–220.
[22] M. E. Levinshtein, S. L. Rumyantsev, G. S. Simin, H. Park, W. C. B. Peatman, and M. S. Shur, Appl. Phys. Lett. **68**, 3138 (1996).
[23] A. K. Kirtania, M. B. Das, S. Chandrasekhar, L. M. Lunardi, G. J. Kua, R. A. Hamm, and L.-W Yand, IEEE Trans. Electron Devices **ED-43**, 784 (1996).
[24] J. A. Copeland, IEEE Trans. Electron Devices **ED-18**, 50 (1971).
[25] M. E. Levinshtein and S. L. Rumyantsev, Semicond. Sci. Technol. **9**, 1183 (1994).
[26] N. D'yakonova, M. E. Levinshtein, and S. L. Rumyantsev, Sov. Phys. Semicond. **25**, 1241 (1991).
[27] B. K. Jones, Adv. Electron. Electron Phys. **87**, 201 (1994).
[28] M. J. Deen, Mater. Sci. Eng., B **20**, 207 (1993).
[29] M. J. Deen, 23rd European Solid-State Device Research Conference (ESSDERC '93), Grenoble, France, (13–16 September 1993), pp. 355–358.
[30] F. N. Hooge, IEEE Trans. Electron Devices **ED-41**, 1926 (1994).
[31] W. L. Kaufmann and A. L. Bergh, IEEE Trans. Electron Devices **ED-15**, 732 (1968).
[32] P. Ma, L. Zhang, B. Zhao, and Y. Wang, IEEE Trans. Electron Devices **ED-42**, 1789 (1995).
[33] X. Y. Chen, M. J. Deen, Z. X. Yan, and M. Schroter (unpublished results).

Downloaded 05 Oct 2003 to 128.46.200.195. Redistribution subject to AIP license or copyright, see http://ojps.aip.org/japo/japcr.jsp